

Arc Phenomena and Gasdynamic Effects due to Interaction of Shock Waves with Magnetic Fields II

H. KLINGENBERG

Institut für Plasmaphysik, 8046 Garching bei München, Germany

(Z. Naturforsch. **24 a**, 540—545 [1969]; received 23 December 1968)

In these experiments continuing the work on interaction published in ¹, the magnetic field, i.e. the retarding force, has been increased. This produces reflected shocks that leave the interaction region, but the steady state could not be achieved.

The already published first part of this paper¹ described arc phenomena and gasdynamic effects produced by interaction of shock-heated plasma flow with a magnetic field perpendicular to the flow direction. Currents of density j flowed through electrodes flush mounted on the inside of the shock tube and connected on the outside. The plasma was therefore subjected to retarding $j \times B$ forces directed opposite to the velocity v and was slowed down. The strong reduction of the plasma velocity resulted in secondary gasdynamic effects, such as reflected shock waves. The high currents necessary for strong interaction could only be produced in the form of arcs. On the other hand, it is known from the literature that only one-dimensional flow has been investigated theoretically because of the mathematical difficulties. With arcs it is difficult to satisfy the simple conditions of one-dimensional theory, such as uniform current distribution in the interaction region. In order to achieve an approximately uniform current distribution in the interaction volume the arc phenomenon was utilized by mounting many electrodes of small surface area alongside and behind one another and short-circuiting the pairs separately, thus producing many arcs alongside and behind one another.

The magnetic field was produced with a crow-barred capacitor bank via coils. The maximum magnetic field strength was about 7 kG. This restricted the maximum interaction strength. The observed gasdynamic effects included reflected shocks still running in the interaction region.

This second part of the paper describes results obtained with the same apparatus, but with a stronger magnetic field above 20 kG that was produced with electromagnetic field coils. With higher

magnetic fields the interaction effect is more pronounced.

From the previous measurements¹, it is known that the current amplitude (and density) is governed by the complex boundary conditions of the plasma-to-electrode transition. This transition is formed by the arc channels leading to the arc spots and by the arc spots themselves. These phenomena could not be interpreted quantitatively, and so the currents have to be measured again because it is not known beforehand whether they become larger or even smaller with higher magnetic fields. But it is not necessary to measure the currents on all electrode pairs again. Measurements on some electrode pairs in each row will do to give sufficient data.

I. Theory

Most comprehensive theoretical investigations were conducted by REBHAN². This author studied the final asymptotic steady state of ideal gases outside the interaction region. Recently, JOHNSON³ investigated the steady and unsteady states of an ideal gas in the interaction region. Figure 1 shows some cases of steady state in the interaction region which are possible according to these theories. P , D , Θ are pressure, density, and temperature respectively related to the values behind the unperturbed primary shock front. M is the flow Mach number. At lower interaction strength P , D , and Θ increase, while M decreases in the interaction region. A rarefaction wave which is still swept downstream by the flow transforms to the states behind the perturbed primary shock after passing through the interaction region. Besides, there may be a secondary contact front. With stronger interaction there is a reflected

¹ H. KLINGENBERG, Naturforsch. **23 a**, 1929 [1968].

² E. REBHAN, Report IPP 3/28, August 1965.

³ M. R. JOHNSON, Phys. Fluids **10**, 539 [1967].



shock front which is still swept downstream by the flow. When the interaction strength is further increased there is a standing reflected shock front in the interaction region.

Finally, the reflected shock travels upstream against the flow outside the interaction region. In these cases P , D , and Θ decrease in the interaction region, while M increases. The latter case is possible even if M is lower than unity.

The results of the previous measurements¹ showed that it is possible to produce reflected shocks. But these shocks were still running in the interaction region and the states were unsteady. Increasing the magnetic field, i.e. the interaction strength, should produce shocks that leave the interaction region in the upstream direction. In this way, the steady state solution of Fig. 1 may serve as a guide for discussing the results.

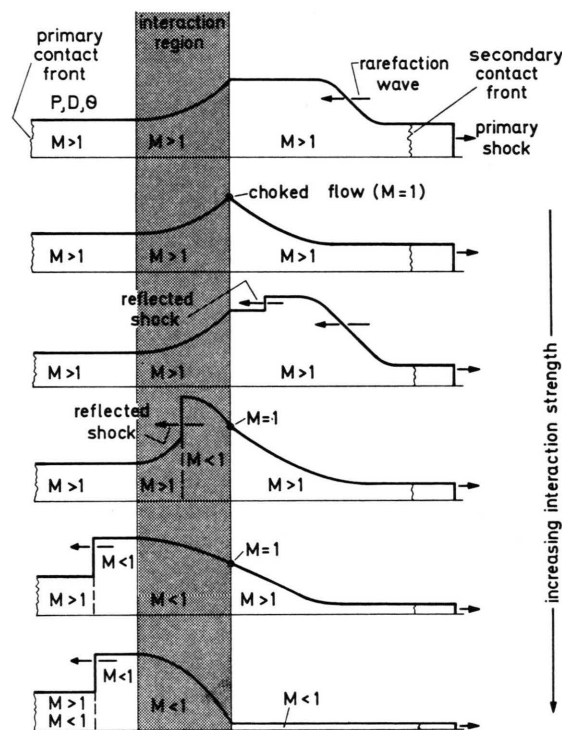


Fig. 1. Cases of asymptotic steady states in the interaction region which are possible according to the theory^{2,3}.

II. Experimental Set-Up

The experimental set-up has already been described in¹. The shock tube is of the diaphragm type. The driving gas is hydrogen (100 atm), and the test gas is argon. The measuring site is 9 m from the diaphragm region. The measuring

chamber is made of plexiglass sections secured between tie plates and has a square internal cross section of (7×7) cm². A sharp cutter is used to cut out the rectangular flow from the circular flow of the shock tube.

Electrodes 4.5 mm in diameter are used in pairs which are short-circuited separately with a copper bridge. The values of 3 m Ω and 0.4 μ Hy can be taken as the mean values for A.C. resistance and inductance respectively for each circuit, cf.¹.

The magnetic field, however, is produced here by big electromagnetic field coils powered by a pulse current of 5 kA for 1 sec. The magnetic field strength was then 21.5 kG and constant during the interaction period. In the interaction region the magnetic field was still uniform to a certain extent.

The currents from the plasma were measured with Rogowski coils mounted on top of the short-circuiting bridges. The signals of the coils were electronically integrated and then recorded by oscilloscopes with the display calibrated directly in units of current. Up to ten coils were used at any one time. The coils agree in sensitivity to within 3%. After electronic integration the sensitivity is 46 mV/kA. The interaction effects were recorded with a drum camera taking streak pictures.

III. Results

1. Results of current measurements

Figure 2* shows as example some oscillograms for two electrode configurations and two initial pressures p_0 . The symbols denoting the electrode configuration are the same as in¹, but they are self-explanatory in any case. For five electrode pairs and $p_0 = 5$ torr the current amplitude is rather high. For 25 electrode pairs the current amplitude is very low at $p_0 = 1$ torr. It is higher at $p_0 = 5$ torr, but the signal is rather irregular in shape. As in previous investigations¹, the integral mean values with respect to time:

$$J = \frac{1}{t_2 - t_1} \int_{t_1}^{t_2} J(t) dt \quad (1)$$

(with $t_2 - t_1$ = pulse length of current) were formed from the oscillograms.

Figure 3 shows these integral mean values in kA. The symbol $\Sigma\Sigma$ denotes the total current (which would come from all electrodes) extrapolated from the measurements on several electrode pairs. Here the current amplitude is higher at higher initial pressures than at lower, as opposed to the results obtained at lower magnetic field strengths¹. (For comparison, some measurements were repeated at lower magnetic fields, but with the big magnetic

* Figure 2, 5, 6 see page 542 a, b.

		\bar{J} in [kA]																	
<div><div>$\uparrow B_0$</div><div>$\rightarrow v$</div></div>		$B_0=215$ kG																	
		$p_0=1$ torr				$p_0=5$ torr				$p_0=10$ torr									
III		III				III				III									
1 ●		.55				.96				.82									
2 ●		.58				.90				1.00									
3 ●		.61				1.16				1.05									
4 ●		.59				1.15				1.21									
5 ●		.57				1.06				.76									
Σ		2.9				5.2				4.8									
per pair on the average		0.6				1.0				1.0									
<div><div>$\uparrow B_0$</div><div>$\rightarrow v$</div></div>		$B_0=21.5$ kG																	
		$p_0=1$ torr				$p_0=5$ torr				$p_0=10$ torr									
II		III				IV				II		III		IV					
1 ○						.20						.65							
2 ●		.53				.25				.68		.51		.59					
3 ○						.28						.36							
4 ●		.42								.32		.49							
5 ○										.32		.63		.27					
$\Sigma \Sigma$		4.5								7.4				7.5					
per pair on the average		0.3								0.5				0.5					
<div><div>$\uparrow B_0$</div><div>$\rightarrow v$</div></div>		$B_0=21.5$ kG																	
		$p_0=1$ torr				$p_0=5$ torr				$p_0=10$ torr									
I		II		III		IV		V		I		II		III		IV		V	
1 ○		.15				—				20				22				21	
2 ●		38						14		34						32		24	
3 ○				.12		.14				.22				.30				.21	
4 ●		.36						—		40						—		.27	
5 ○				.15		.08						.33				.30		.48	
$\Sigma \Sigma$		5.0								7.5				7.5					
per pair on the average		0.2								0.3				0.3					
<div><div>$\uparrow B_0$</div><div>$\rightarrow v$</div></div>		$B_0=5.6$ kG				$B_0=11.2$ kG				$B_0=21.5$ kG									
		$p_0=1$ torr																	
I		II		III		IV		V		I		II		III		IV		V	
1 ○		.24				.28				.23				.20				.15	
2 ●		38						.33		42				.22		.38			
3 ○				.21		.23				.21				.18				.12	
4 ●		35						—		29				.23		.36		.14	
5 ○				—		.26				.33				.24				.15	
$\Sigma \Sigma$		7.0								6.3				5.0					
per pair on the average		0.28								0.25				0.2					

Fig. 3. Results of current measurements. Arithmetic mean values of the integral mean values with respect to time of the current in kA. The symbol $\Sigma \Sigma$ denotes the extrapolated total current which would flow from all electrode pairs.

field coils. These values of current amplitude per electrode pair or of the total current agree with the values from previous measurements¹.)

For five electrode pairs and for $p_0 = 1$ torr the current at the higher magnetic field of 21.5 kG is nearly the same as in the previous case of 6.8 kG¹, but higher than in the previous case for $p_0 = 5$ torr and $p_0 = 10$ torr.

For 25 electrode pairs and for $p_0 = 1$ torr the current is smaller than at lower magnetic field strengths, especially at the last electrode rows. For $p_0 = 5$ torr and $p_0 = 10$ torr the current is nearly the same as for $p_0 = 1$ torr in the previous case. Only at $p_0 = 10$ torr is the current thus higher than in the previous investigations.

As in the previous investigation, see Fig. 3 in¹, the currents per electrode pair decrease with the number of electrodes. The total current here for 15 electrode pairs is as high as for 25 electrode pairs.

Figure 4 shows the current values for one electrode pair with increasing magnetic field. In this case the current rises.

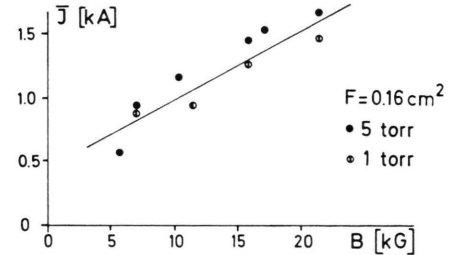


Fig. 4. Current for one electrode pair as function of the magnetic field. (F = surface area of electrode.)

Arc spots were always observed; for detailed discussion see¹.

The internal resistance was also given in¹. It has the same value here of about 400 m Ω per circuit for 25 electrode pairs.

2. Calculation of the interaction parameter

The interaction strength can again be estimated with the interaction parameter N :

$$N = \frac{j \cdot B_0 \cdot L}{p_1 + q_1 v_1^2} \quad (2)$$

where $j \cdot B_0 \cdot L$ is the retarding force per unit area (L = interaction length), and $p_1 + q_1 v_1^2$ is the total hydrodynamic pressure of the unperturbed flow. The total hydrodynamic pressure of the flow can be calculated⁴. The current density is not known, of course, but it is reasonable to assume that it is uniform across the channel (vertical to the flow direction) if one or more rows of five electrode pairs are used¹.

Then the current J can be expressed as

$$J = a \int_0^L j dx \quad (3)$$

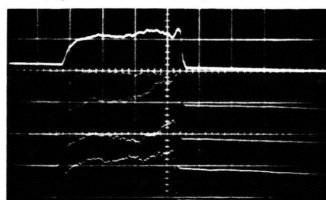
where a is the width of the channel. In this case the retarding force can be written as

$$B_0 \int_0^L j dx \quad (4)$$

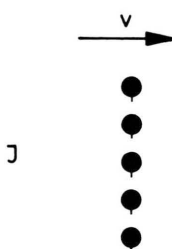
⁴ H. KLINGENBERG and H. MUNTENBRUCH, Report IPP 3/45, November 1966.

Rogowski coils type II

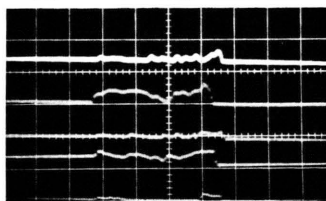
$p_o = 5 \text{ torr}$ $B_o = 21.5 \text{ kG}$



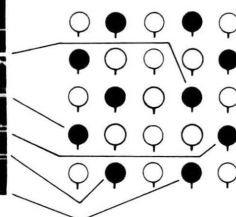
0.05V/div ; 100 μsec /div



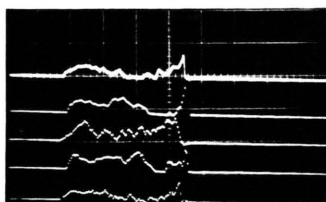
$p_o = 1 \text{ torr}$ $B_o = 23.9 \text{ kG}$



0.05V/div ; 50 μsec /div



$p_o = 5 \text{ torr}$ $B_o = 21.5 \text{ kG}$



0.05V/div ; 100 μsec /div

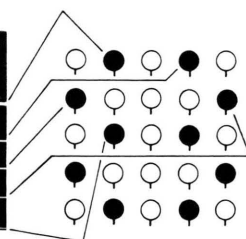


Fig. 2. Oscillograms of the current.

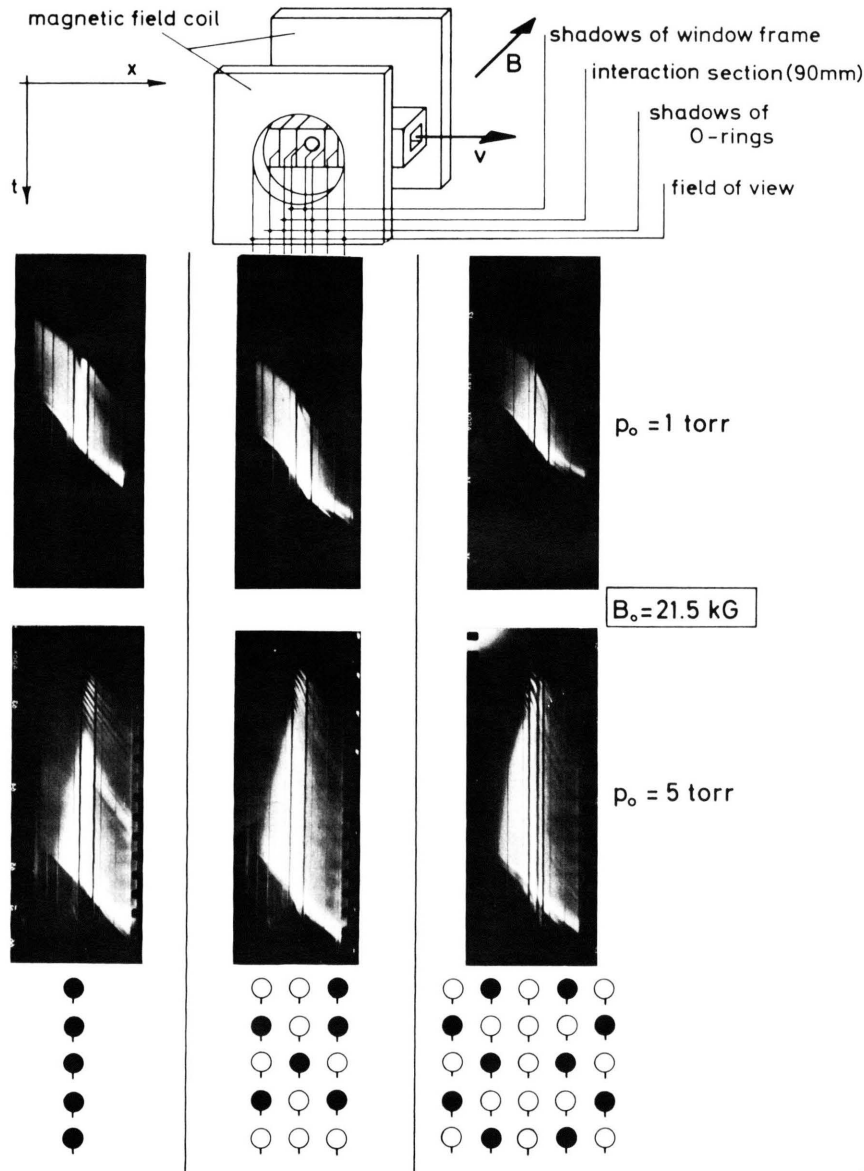


Fig. 5. Streak photographs for two initial pressures and three electrode configurations. The incandescence of the unperturbed plasma has been stopped down for the bottom pictures at $p_0 = 5$ torr.

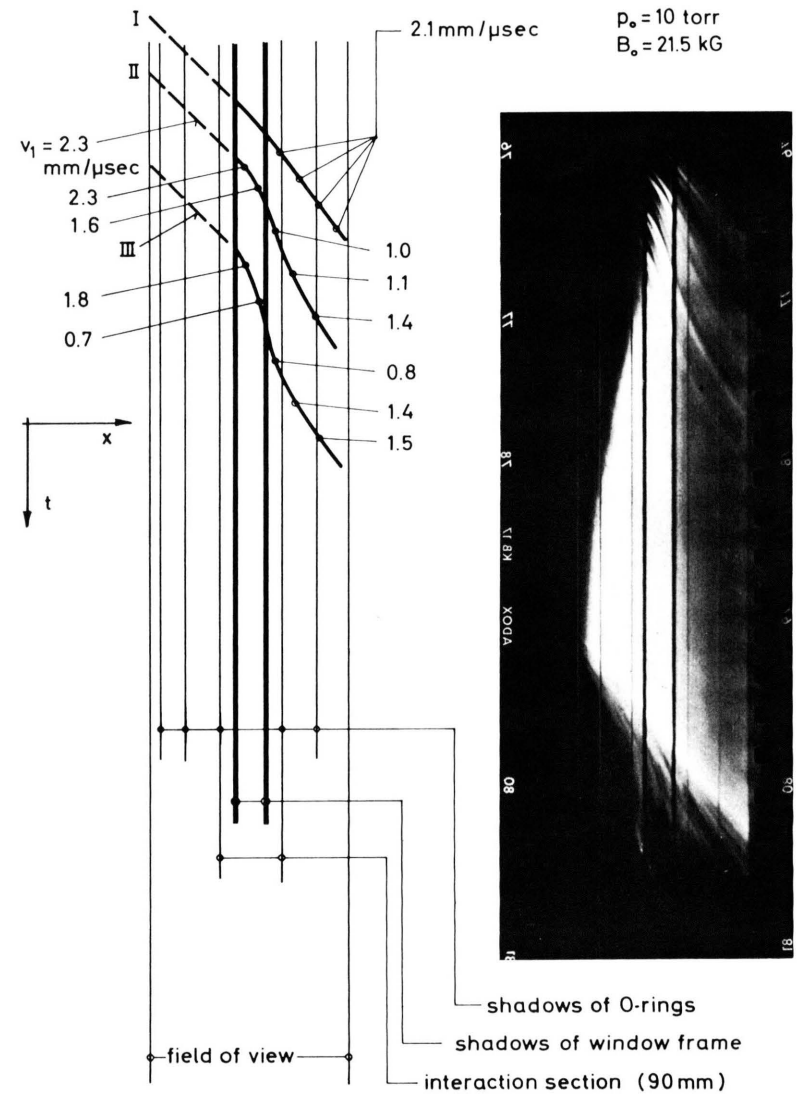


Fig. 6. Streak picture for $p_0 = 10$ torr with 25 electrode pairs. Evaluated were the velocities of the secondary fronts thus giving values of flow velocities at several points. The local velocity of sound in the unperturbed plasma is 1.6 mm/ μ sec. The incandescence of the unperturbed plasma has been stopped down.

or N as

$$N = \frac{\bar{J} \cdot B_0/a}{p_1 + q_1 v_1^2} \quad (5)$$

where \bar{J} is the measured integral mean value of the current.

(Here only the external magnetic field strength B_0 is taken into account. This is possible since the magnetic Reynolds number

$$R_m = \mu_0 j L / B_0 \quad (6)$$

is smaller still by a factor of about 3 than in the previous measurements¹, because the current does not increase with the magnetic field. From this point of view this is an advantage. For instance, with 25 electrode pairs and $B_0 = 21.5$ kG R_m is 0.06.)

As the results of the current measurements show, \bar{J} is not increased by using more small electrodes in the flow direction. Using more electrodes will therefore not increase the interaction strength, see Table 1.

p_0 torr	$B_0 = 6.8$ kG * number of electrode pairs			
	5	10	15	25
0.5				0.7
1	0.2	0.3	0.4	0.5
2				0.3
5				0.2
10				0.04
$B_0 = 11.2$ kG				
1				0.6
$B_0 = 21.5$ kG				
1	0.6		1	1.1
5	0.4		0.6	0.6
10	0.2		0.3	0.3

* From previous measurements, cf. ¹.

Table 1. Values of interaction parameter N , cf. (2), (5).

Table 1 shows the calculated values of N . For comparison the values of N given previously¹ for $B_0 = 6.8$ kG are also included. The N values are comparable only at the same shock Mach number, i.e. in our case at the same initial pressure p_0 since the driver gas pressure is constant.

At higher magnetic fields N is always higher for the same initial pressure. Most pronounced is the difference at $p_0 = 10$ torr. According to the theory the reflected shocks should now run upstream against the flow and leave the interaction region, see Fig. 1.

3. Results of drum camera measurements

Figure 5 shows some streak pictures with p_0 and the electrode configuration as parameters.

At $p_0 = 1$ torr a reflected front is not clearly visible. At the bottom left, however, fairly strong incandescence can be observed, this being an indication that a reflected front collides with the primary contact front. It can also be seen clearly that the incandescence of the plasma decreases strongly at the top right. The primary shock front and the gas behind it cease to be incandescent after passing through the interaction region. In the centre a dark front is observed.

At $p_0 = 5$ torr the reflected front is clearly visible. (The incandescence of the unperturbed plasma was stopped down.) It runs out of the interaction region against the flow into the unperturbed gas which has been compressed behind the primary shock before this shock entered the interaction region.

Also clearly visible are the secondary fronts, c.f. ¹ These fronts are produced when very small particles of impurities (dust from the diaphragms) are carried along by the streaming gas. The velocity of these fronts is, according to the previous measurements¹, roughly equivalent to the flow velocity of the plasma behind the primary shock. It is thereby possible to determine approximately the flow velocity, this being very difficult otherwise. Figure 6 shows as an example a streak picture at $p_0 = 10$ torr with 25 electrode pairs. Again the reflected front can be clearly seen (the incandescence of the unperturbed plasma has been stopped down), but the secondary fronts as well. Thus, the flow velocity could be evaluated at some points. The flow is slowed down in the interaction region to values of, for instance, 0.7 mm/ μ sec. The local velocity of sound in the unperturbed plasma is 1.6 mm/ μ sec. It may even be a little higher here because of the higher temperature in the region where the current is flowing. Therefore the flow is subsonic behind the reflected front. This is proof that the reflected front is a shock front. Behind the interaction the flow velocity again increases towards supersonic values. This indicates the existence of rarefaction waves. These waves accelerate the plasma to the velocity governed by the shock Mach number of the perturbed primary shock after passing through the interaction region, see Fig. 1.

Furthermore, the measurement shows that the state is still unsteady in the interaction region, at least for the first 100 μ sec.

A device for differentiating curves was used to evaluate the streak pictures with respect to the

velocity of the reflected fronts. The results are shown in Fig. 7. For $p_0 = 5$ torr the experimental points refer to all three electrode configurations in Fig. 5 (top). For $p_0 = 10$ torr, the points refer to

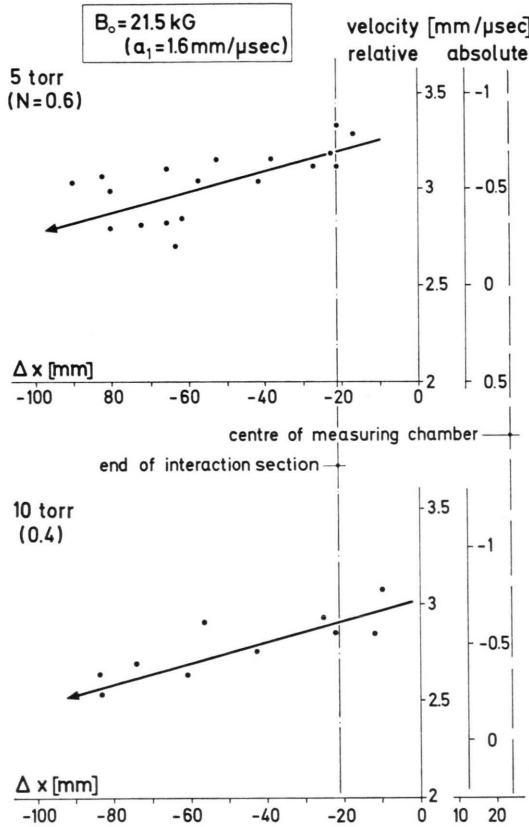


Fig. 7. Velocities of reflected fronts. The relative values refer to the flow velocity. The arrows indicate the development with time.

the configuration of 25 electrode pairs. The direction of the flow velocity v_1 behind the primary shock front is taken as positive. The relative values refer to the calculated (and measured) flow velocity which the plasma has behind the unperturbed primary shock front. The arrows indicate the development with time. The Mach numbers of these fronts vary between 2.0 and 1.5. There is still a change of the velocity with time.

IV. Discussion

The results of the current measurements only confirm the results of the previous investigations¹, viz. that the complex boundary conditions in the

transition from the plasma to the arc spots determine the current amplitude (and density) and that no predictions can be made. The currents have therefore to be measured again for every change of parameter.

The current amplitude cannot be increased, for instance, by increasing the magnetic field strength, at least at low initial pressures and with more than one electrode pair. The complex boundary conditions are presumably even more complex with higher magnetic fields. For instance, the retrograde motion indicated by the results of the previous measurements should become more pronounced. This higher complexity may explain the more irregular current behaviour, see Fig. 2.

On the other hand, the decrease of the current for $p_0 = 1$ torr and 25 electrode pairs at the last electrode rows indicates that the slowing down of the plasma has an influence.

With higher magnetic fields the retarding $j \cdot B$ force or the interaction parameter N is higher at the same initial pressure.

According to the theory (see Fig. 1) there are reflected fronts leaving the interaction region in the upstream direction, while at lower interaction strengths they remain in the interaction region¹. These reflected fronts are most probably shock waves. This is confirmed by the fact that the measured flow velocity behind these fronts is subsonic. There is, however, reason for concluding that relaxation effects are again involved, and so, strictly speaking, the observed luminous fronts are not the shock fronts. One reason is that the "sharpness" of the front diminishes with decreasing initial pressure. This has already been described in¹. But here the reflected shock fronts run into the unperturbed plasma produced by the unperturbed primary shock. The properties of this plasma are well known⁴. In this way, relaxation effects of plane shock waves running into a plasma can be studied.

The dark region observed behind the primary shock at $p_0 = 1$ torr, see Fig. 4, is probably a contact front.

The existence of rarefaction waves is proved by the acceleration of the flow behind the subsonic region.

V. Concluding Remarks

The results of these investigations show that it is possible to utilize arc phenomena to produce

strong interaction effects, such as reflected shocks and rarefaction waves.

Other experimental investigations, mainly quantitative, are necessary, however, to prove that the observed reflected fronts are plane shock fronts and to determine all flow parameters. In addition, relaxation effects behind shock waves in plasmas can be studied.

Only then can the experimental results be reasonably compared with the theory. But the steady state cannot be achieved, as the results show. Therefore the transient part of the theory of JOHNSON² must be taken as a basis. However, the assumption made in this theory that the current density can be ex-

pressed in terms of $\sigma \cdot \nabla \cdot B$ is not valid. Furthermore, ionization effects have to be taken into account. More experimental and theoretical investigations are therefore required.

The author wishes to thank Prof. R. WIENECKE for encouragement and for his continued interest in this work. He is indebted to his colleagues Mr. ZIMMERMANN for his help with the measurements and Mr. SARDEI for discussions concerning the theory. He is grateful to Mr. SCHMID, Mr. STEFFES and Mr. LOEBEL for technical assistance.

This work has been undertaken as part of the joint research programme of the Institut für Plasmaphysik and Euratom.

Higher Harmonics Generation in Weakly Ionized Plasmas in Time-Varying Crossed Fields

WOLFGANG STILLER* and GÜNTER VOJTA

Arbeitsstelle für Statistische Physik der Deutschen Akademie der Wissenschaften zu Berlin
705 Leipzig, DDR

(Z. Naturforsch. **24 a**, 545—555 [1969]; received 21 November 1968)

The linearized Boltzmann equation of kinetic theory for the electrons of a weakly ionized plasma under the action of an alternating electric field $\mathbf{E} = \cos \omega t \{E_x, E_y, E_z\}$ and a circularly polarized magnetic field $\mathbf{B}^R = B \{\cos \omega_B t, \sin \omega_B t, 0\}$ is solved. The direction-dependent part $f^1(\mathbf{r}, \mathbf{v}, t)$ of the distribution function contains especially higher harmonics with frequencies $2\omega_B$, $\omega \pm \omega_B$, $\omega \pm 2\omega_B$. These overtone frequencies are generated — unlike the higher harmonics obtained by Margenau and Hartman — by a cross drift mechanism and are present even if the isotropic part f^0 of the electron distribution function is assumed to be time-independent. The physical meaning of the various contributions to the distribution function f^1 is discussed in detail.

1. Introduction

The influence of crossed electric and magnetic external fields on plasmas has been studied for several reasons and with different methods. For example, it is interesting to learn at which electric field strengths the breakdown in a high-frequency low pressure gas discharge starts. Furthermore, it is important to study the plasma particle motion in crossed field geometries in order to get information about a possible particle acceleration. This is of interest in cosmic ray physics, electron and ion optics

etc. Finally a large amount of effort has been devoted to the examination of appropriate crossed field configurations for an effective heating and a stable confinement of high temperature plasmas. Often it is sufficient and less expensive to examine these problems in suitable model plasmas, e.g. using the weakly ionized regions of low pressure discharges¹.

Many investigations have been performed in which the crossed fields are assumed to be static. With respect to the applications mentioned it is also important to study the plasma behaviour if the ex-

* Based on a part of a thesis submitted to the Mathematisch-Naturwissenschaftliche Fakultät der Karl-Marx-Universität Leipzig in partial fulfillment of the requirements for the degree of Dr. rer. nat.

¹ F. KARGER, Z. Naturforsch. **22 a**, 1890 [1967].